Ductility and cracking behavior of reinforced coconut shell concrete beams incorporated with coconut shell ash

Article · March 2022

DOI: 10.1016/j.rineng.2022.100401

CITATIONS
4

READS
111

3 authors, including:

Trokon Herring
Pan African University Institute for Basic Sciences, Technology and Innovation
5 PUBLICATIONS **9** CITATIONS

SEE PROFILE

Results in Engineering 14 (2022) 100401

Contents lists available at ScienceDirect

Results in Engineering

journal homepage: www.sciencedirect.com/journal/results-in-engineering

Ductility and cracking behavior of reinforced coconut shell concrete beams incorporated with coconut shell ash

Trokon Cooper Herring [a,*], Timothy Nyomboi [a], Joseph N. Thuo [b]

[a] Department of Civil and Construction Engineering, Pan African University Institute for Basic Sciences, Technology and Innovation, Nairobi, Kenya
[b] Department of Building and Civil Engineering, Dedan Kimathi University of Technology, Nyeri, Kenya

ARTICLE INFO

Keywords:
Coconut shell particles
Coconut shell ash
Strength
Ductility
Shear

ABSTRACT

Coconut shell concrete beams containing coconut shell ash are a feasible alternative to traditional reinforced concrete beams in structural applications. Coconut shells in reinforced concrete beams are essential in earthquake-prone areas because of their ductility properties, which contribute to enhancing earthquake resistance. This research investigates the flexure, ductility, shear, and cracking behavior of reinforced concrete beams made from the incorporation of a minimum quantity of untreated coconut shell particles (CSP) at 5% substitution of coarse aggregate (CA) modified with coconut shell ash (CSA) at 10% substitution of Ordinary Portland cement (OPC). Two beams were evaluated for flexural, strain, ductility, and cracking behavior. In contrast, the other two were evaluated for flexural, shear, strain, ductility, and cracking behavior by repositioning the loading point to the distance of 200 mm close to the support. In comparison to control beams evaluated for flexural, shear, strain, ductility, and cracking behavior, the ductility ratio of concrete beams with 10% CSA and 5% CSP improved by 8.8%. The ductile improvement was observed with a 17.3% decrease in flexural load. The shear capacity of reinforced concrete beams with 10% CSA and 5% CSP improved compared to the reference literature in the study. Finally, it was discovered that combining 10% CSA and 5% CSP in reinforced concrete beams can improve ductility without significantly reducing ultimate failure load.

1. Introduction

Aggregates are a substantial component of concrete mixes and have a considerable impact on the structural performance of concrete [1]. Because of urbanization and industrialization, aggregate consumption has risen fast in recent decades. Due to aggregates' high consumption, its sources are becoming depleted, and prices are rising. The use of lightweight aggregate concrete saves 10–20% of the total cost of concrete and eliminates the need for conventional aggregate depletion [2]. To reduce weight and improve thermal insulation, lightweight concrete (LWC) has become increasingly popular [3,4].

The use of coconut shell (CS) as a lightweight aggregate to produce lightweight structural concrete (LWC) has been explored by the literature [1,4–8]. High-rise structures in earthquake-prone areas benefit greatly from the ductility feature, which increases earthquake resistance. In the aftermath of earthquakes, structural engineers play a critical role [9]. Gunasekaran et al. [1] experimented with reinforced lightweight coconut shell concrete beams under flexure and concluded that coconut shell concrete beams flexural loadings proved that they had good ductility and could reach their maximum capacity. Prakash et al. [9] experimented with coconut shells and observed that all beams with coconut shells failed in a ductile way with a considerable deflection that was within the allowable range as per IS 456 (2000). Other lightweight aggregates, such as palm kernel shells and waste tire rubber, have also improved concrete ductility compared to normal concrete [10,11].

Ordinary Portland cement (OPC) is usually expensive, one of the most important components, and produces CO_2 [13]. The cement industry has reduced cement output and partially replaced cement with alternative cementitious materials due to environmental and social concerns about sustainability and energy conservation. There is an ever-increasing need for pozzolans to replace cement in concrete, and the vast production of cement is causing environmental degradation [12]. More so, pozzolanic materials in concrete are rapidly becoming a must-have strategy for addressing environmental concerns associated with cement manufacture [14,15]. Various studies have been conducted to determine the viability of using coconut shell ash (CSA) as an alternative cement replacement material. Coconut Shell Ash is a viable substitute for Ordinary Portland cement (OPC) due to its pozzolanic

* Corresponding author.
E-mail address: trokonh@yahoo.com (T.C. Herring).

https://doi.org/10.1016/j.rineng.2022.100401
Received 15 February 2022; Received in revised form 10 March 2022; Accepted 22 March 2022
Available online 29 March 2022

quality, which improves the cementitious composite strength [13]. Coconut shell ash (CSA) is created when crushed coconut shells are burned. Adeala et al. [14] completed a report on the use of coconut shell ash in concrete as a partial substitute for ordinary Portland cement. The findings showed that replacing OPC with CSA from 5% to 15% is recommended for structural concrete.

Past research on the application of CSA in concrete has mostly focused on its engineering properties. On the other hand, many studies have also been carryout on reinforced coconut shell lightweight concrete beams with a limited investigation on the structural behavior of reinforced concrete beams with the incorporation of CSA and minimum content of CSP. This research investigates the flexure, ductility, shear, strain, and cracking behavior of reinforced concrete beams made from incorporating a minimum quantity of untreated coconut shell particles (CSP) at 5% of coarse aggregate (CA) modified with coconut shell ash (CSA) at 10% of OPC. In order to achieve construction sustainability, the construction industry should consider enhancing the ductility properties of reinforced beams. Incorporating CSP and CSA in reinforced concrete beams could increase ductility while lowering pollution levels.

Therefore, the critical contributions of this research include:

(i) Investigation of the workability and compressive strength of concrete made from incorporating 5% of untreated coconut shell particles (CSP) modified with 10% coconut shell ash (CSA).
(ii) Examination of the flexure, ductility, strain, and cracking behavior of reinforced concrete beam made from incorporating 5% of untreated coconut shell particles (CSP) modified with 10% coconut shell ash (CSA).
(iii) Assessment of the flexure, ductility, strain, shear, and cracking behavior of reinforced concrete beam made from incorporating 5% of untreated coconut shell particles (CSP) modified with 10% coconut shell ash (CSA).

2. Research methods

2.1. Material

2.1.1. Concrete material properties

Ordinary Portland Cement (OPC) class 42.5 was utilized, which met the standard criteria [17]. The specific gravity of OPC and CSA were 3.11 and 2.06, respectively. CSA was categorized as a lightweight because its specific gravity was less than 2.4 [16]. The total of (SiO_2 + Fe_2O_3 + Al_2O_3) in CSA was greater than 70%, meeting the ASTM C618 criteria for Class N pozzolanic material (Table 1). Crushed stone aggregate with a maximum size of 20 mm and natural sand were utilized as coarse and fine aggregate. As per [17,18], coarse aggregate (crushed stone) with a maximum size of 20 mm and fine aggregate (natural sand) were used. Fine and coarse aggregates had a specific gravity and water absorption value of 2.57 and 2.14%, 2.53 and 3.33%, respectively. CSP with a maximum particle size of 20 mm had a specific gravity of 1.28 and water absorption of 29.67%. Fine aggregates (FA), coarse aggregates (CA), and CSP grading are depicted in Figs. 1–3. CA and CSP had aggregate crushing value (ACV) and aggregate impact value (AIV) of 16.74% and 2.26%, and 12.69% and 8.14%, respectively. Hence ACV and AIV values obtained for CA and CSP conform to the BS 812 standard.

Table 1
Chemical Composition of cement and coconut shell ash.

Component	Cement (%)	CSA (%)
SiO_2	25.17	52.55
AL_2O_3	5.64	13.74
Fe_2O_3	2.63	7.65
Cao	61.86	3.55
MgO	–	1.60
Na_2O	0.08	0.47
K_2O	0.65	2.35
MnO	0.02	0.08
SO_3	2.79	0.57
Loss on ignition	2.81	7.69

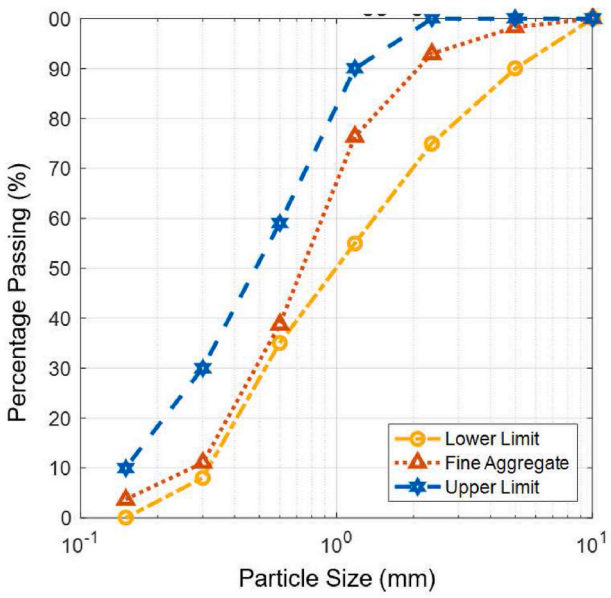

Fig. 1. Fine Aggregate gradation.

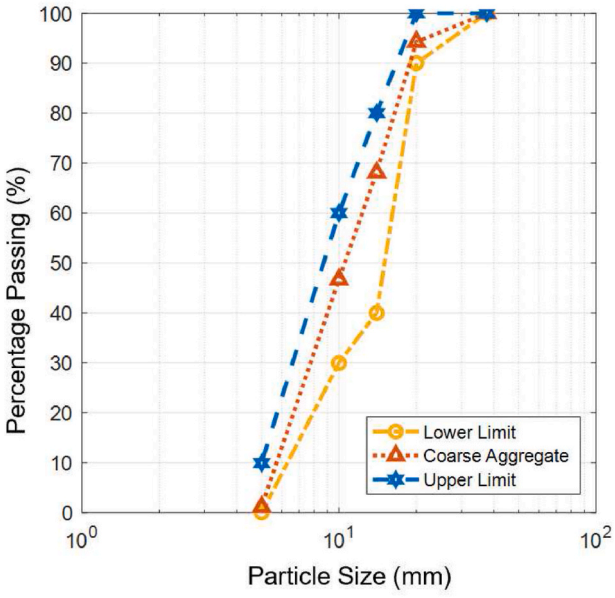

Fig. 2. Coarse Aggregate gradation.

2.1.2. Concrete

The concrete class of 30 was used, according to the British Research Environment (BRE). The design mix that was used is shown in Table 2, with slump values of 30–60 mm and a water-cement ratio of 0.55. The four mixes utilized to assess concrete compressive strength were control concrete (0), mix with 5% coconut shell particles (CSP5), mix with 10% coconut shell ash (CSA10), and mix with a mixture of 10% coconut shell ash and 5% coconut shell particles (CSA10&CSP5). The compressive strength tests were conducted using small cubes molds with the volume of 1 m^3 cubic millimeter cured in water for 7, 28, 56, and 90 days to establish a knowledge of the strength growth with the introduction of CSA as a pozzolanic material. Because reinforced concrete members

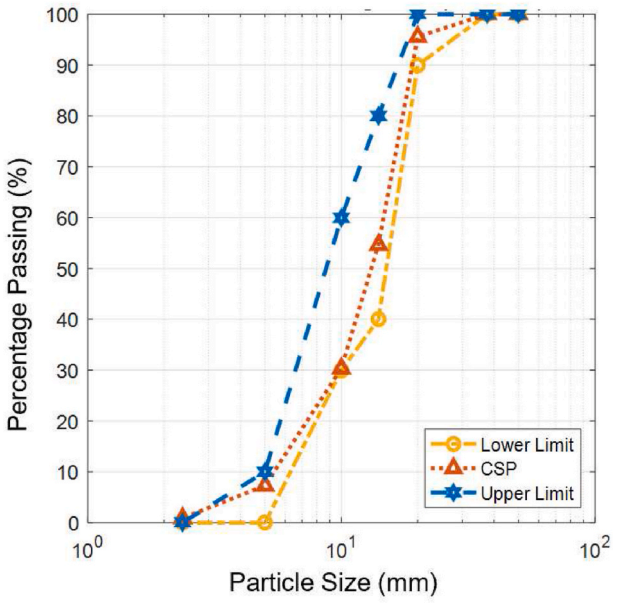

Fig. 3. Coconut Shell Particles gradation.

Table 2
Concrete mix.

Specimen ID	Cement	CSA	Sand	Coarse aggregate	CSP	Water to cement ratio
	kg/m^3	kg/ m^3	kg/ m^3	kg/m^3	kg/ m^3	w/b
Control	381.82	0	759.44	1048.7	0	0.55
CSP5	381.82	0	759.44	996.26	52.44	0.55
CSA10	343.64	38.18	759.44	1048.7	0	0.55
CSA10&CSP5	343.64	38.18	759.44	996.26	52.44	0.55

must be ready for use and service after the 28 day curing period, the beams were examined. Control and a mix with a combination of 10% CSA and 5% CSP (CSA10&CSP5) were considered for the beams testing. Workability tests were performed on fresh concrete as per the standard [19,20].

2.1.3. Steel bars and links

Reinforcing bars of 8 mm and 12 mm diameter were tested up to failure following [21] using the Universal Testing Machine (UTM). Three specimens were used for each steel reinforcement bar diameter in the experiments. In Table 3, T8 and T12 average ultimate strengths were 724.88 MPa and 666.54 MPa, respectively. T8 had a greater average yield strength of 548.88 MPa, as expected, than T12, which had a value of 492.02 MPa. The ultimate strength to yield strength ratio (fu/fy) was between 1.32 and 1.35. The minimum strain hardening requirement (fuk/fyk) for ribbed reinforcing bars is 1.05 [22]. Yield strength is an important steel attribute in assuring material quality for engineering applications. T12 bars had a decreased yield when compared to T8 bars. The findings are consistent with other researchers' findings [23]. After yield, fu/fy values larger than 1.05 are predicted to undergo significant strain hardening, which increases the ductility of steel [24,26]. This was visible in the steel bars used in this investigation because all fu/fy for were larger than 1.05. Steel tensile strength values appeared to meet standards for concrete reinforcing applications requiring ductility characteristics.

2.2. Beam setup and testing

2.2.1. Specimen preparation and casting

Four 150 mm × 200 mm x 2000 mm beams were tested in accordance with [24] to determine the flexure, shear, ductility, and mechanism of failure of concrete containing CSA and CSP. The beams for Class 30 concrete were designed in accordance with BS [28]. Flexure beams were denoted by the abbreviations FBC and FBM. The shear and flexure beams were designated SFBC and SFBM1, respectively. The beams were formed using construction plywood. All steel reinforcement schedules, sizing, and bending was done in compliance with the standard [29]. Steel reinforcement strain was measured using 118.5 ± 0.5 Ω gage resistance strain gauges.

The mid-span tension bars and the shear links 225 mm from the loading point were smoothed with a bench grinder for strain gauge installation. The strain gauges were carefully embedded on steel bars with glue then covered with waterproof material for protection before casting. The beam samples were cast horizontally in the plywood shape. Compaction with a poker vibrator was then performed. The specimens were demolded without causing any damage after 24 h. They were then moist-cured to achieve uniform curing by covering them with sand and damp gunny bags. The samples were maintained in the laboratory for 28 days at room temperature and with humidified air.

2.2.2. Test setup and instrumentation

The beams for flexural testing were built conceptually in Fig. 4 and realistically in Fig. 5. A dial gauge was installed on the beam bottom center surface for mid-span deflection recording. When the test began, the loading point was placed at a distance sufficient to achieve only flexure failure in the beam. The load was applied constantly at pressure by a 400 kN hydraulic jack until the maximum load resulting in failure was reached. The applied load was measured using a load cell with a capacity of 200 kN. For each load increment, deflections were measured using a dial gauge coupled to a data logger. The maximum load was determined. To determine the specimen ductility, load-deflection curves were plotted. The beams were inspected to understand how the cracks were developing. After completing the test, beams were examined to determine deflection, crack spacing, crack patterns, and failure modes. To achieve flexure and shear failure, loads were applied to the other beams at a distance of 200 mm from the supports. Figs. 6 and 7 show the reinforcement details and test setup for beams tested for ductility, cracking behavior, shear, and flexure performance. This distance was obtained by utilizing the shear reinforcement criteria specified during beam design. The loads were placed this far away from the supports in order to test the flexural, ductility, and shear properties of SFBC and SFBM, respectively.

Table 3
Tensile Strength results of T8 and T12.

Sample name	Diameter (mm)	Ultimate Strength (MPa)	Average Ultimate Strength (MPa)	Yield Strength (MPa)	Average Yield Strength (MPa)	Average (fu/fy)
$T12_A$	12	651.45	666.54	459.93	492.02	1.35
$T12_B$	12	676.75		507.14		
$T12_C$	12	671.42		509.00		
$T8_A$	8	724.50	724.88	569.89	548.88	1.32
$T8_B$	8	725.64		507.11		
$T8_C$	8	724.51		569.65		

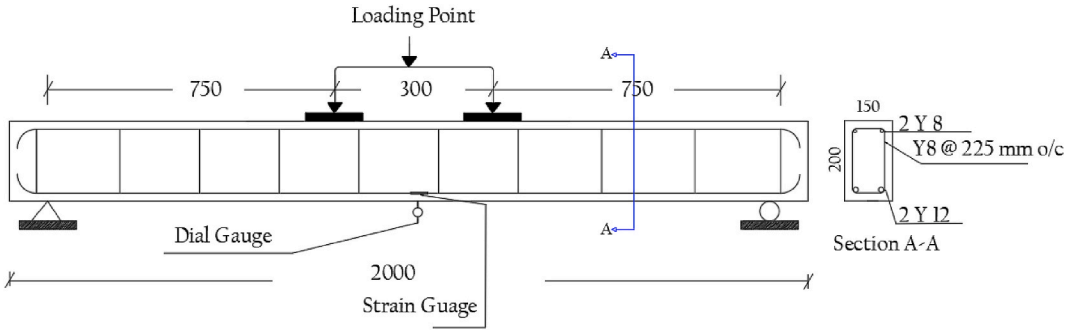

Fig. 4. Flexural beams reinforcement details.

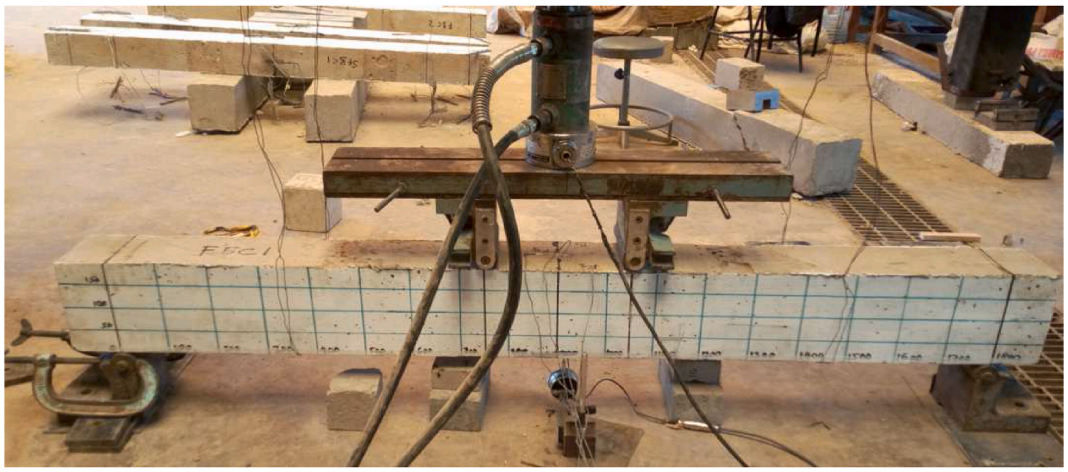

Fig. 5. Flexural beams test setup and instrumentation.

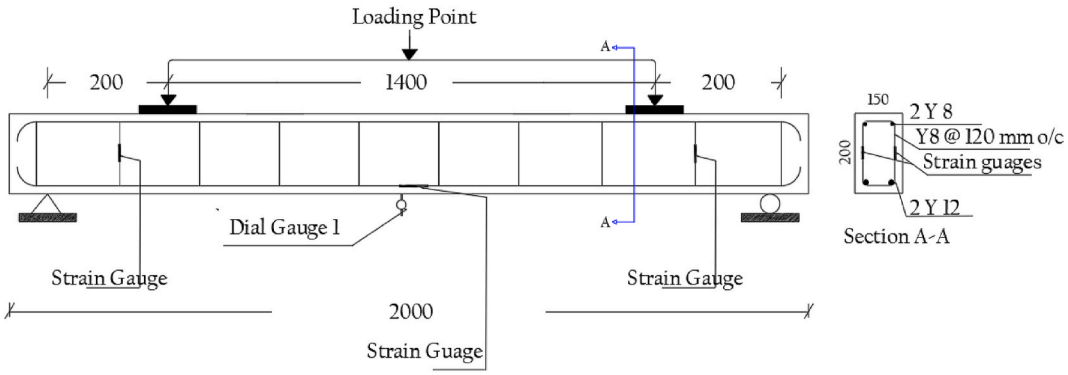

Fig. 6. Flexural and shear beams reinforcement details.

3. Results and discussion

3.1. Workability

When CSA and CSP are used in concrete production, the workability for the fixed water-cement ratio is reduced. Fig. 8 demonstrates the workability of control, 5% CSP, 10% CSA, and the combination of 10% CSA and 5% CSP concrete mixes. As 10% CSA and 5% CSP5 were mixed, concrete workability decreased much more when compared to control and other individual percent substitutions. CSP has a low specific gravity, thus occupying more surface area. CSP can store water as an internal reservoir due to its porous nature and high-water absorption, needing extra water for increased workability [25]. The absorbent nature and particle fineness of CSA may have also contributed to the reduction in workability. CSA and other pozzolanic components stiffen concrete mixtures [26], which may have resulted in a further loss of workability. Fig. 8 also shows that 10% CSA had a greater impact on slump and compaction factor reduction than the 5% CSP. This is also owing to the fact that Concrete contains a lot more CSA than CSP content.

3.2. Compressive strength

As seen in Fig. 9, the compressive strength of all mixes increased with age. At 28, 56, and 90 days, the compressive strength of the combination of 10% CSA and 5% CSP is 30.82%, 39.54%, and 40.39%, respectively, higher than at 7 days. At 28, 56, and 90 days, the compressive strength of the individual mixtures of 10% CSA, 5% CSP, and control concrete is:

Fig. 7. Shear and flexural beams test setup and instrumentation.

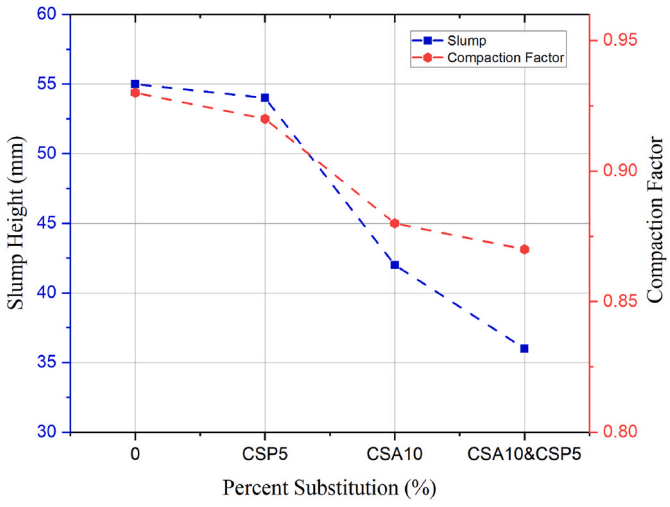

Fig. 8. Workability of control and modified concrete.

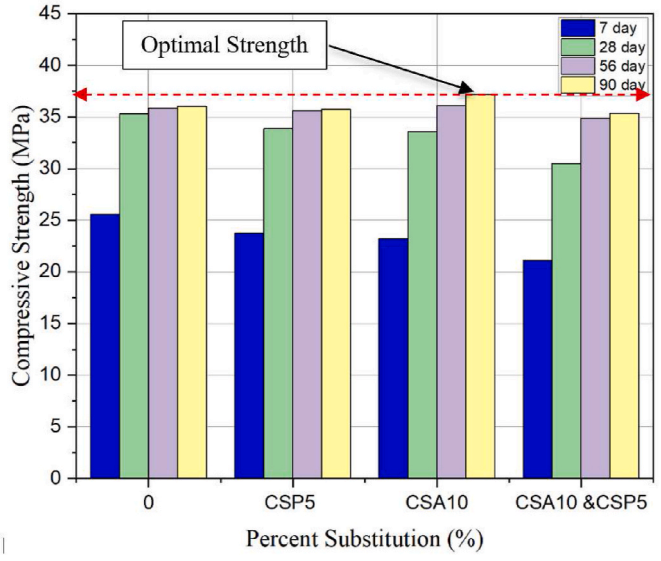

Fig. 9. Compressive strength of control and modified concrete.

30.95%, 35.73%, and 37.63%; 30.1%, 33.43%, and 33.61%; 28%, 28.69%, and 28.88%, respectively, higher than that of the seven (7) day strength. Beyond 28 days, it is obvious that concrete containing CSP and CSA grows in compressive strength more than control concrete. The continuous hydration of Portland cement and the CSA-delayed pozzolanic reaction result in a denser microstructure. Coconut shell particles collect water and hold it in their pore structures, which act as reservoirs for long-term concrete curing and strength development [8].

It's also worth noting that concrete with 10% CSA had the optimal strength in compression compared to control, 5% CSP, and the combination of 5% CSP and 10% CSA after 56 and 90 days of curing. This is because of $Ca(OH)_2$ reaction with SiO_2 was triggered beyond the 28-day curing period, thus releasing a large about of C–S–H gel. The compressive strength of the combination of 10% CSA and 5% CSP was slightly lower than control at 56 and 90 days of curing. The majority of the blame lies with the failure of the link between the coconut shell aggregate and the hardened cement paste. Compared to control concrete, the combined inclusion of 10% CSA and 5% CSP resulted in compressive strength of 35.4 MPa, which was 3.23% lower than control concrete after 90 days. The compressive strength output obtained in this research differ from those of [27] who studied the comprehensive study of waste coconut shell aggregate as raw material in concrete. The difference can be attributed to the presence of the CSA SiO_2, which reacts perfectly with cement-free lime, and the CSP grading size, which occupies less surface area.

3.3. Flexural strength and deformation

3.3.1. Load deflection and ductility behavior

Fig. 10 depicts the load-deflection behavior of the control beams (FBC) and beams 10% CSA and 5% CSP (FBM) failing in flexure. Cracking begins at the bottom of the beam portion, where the cracks originate, then spreads swiftly to the beam's top as the applied stress increases, causing the beam to fail completely. FBC beam was 17.3% higher than FBM beam at ultimate loads. The addition of 10% CSA in FBM may have lowered strength due to SiO_2 not reacting with $Ca(OH)_2$ at the 28-day curing period. Also, adding 5% of CSP resulted in a decrease in FBM strength. The loss in flexural strength of coconut shell concrete is thought to cause this behavior [33]. This reduction is due to weak bonding between coconut shell particles and other concrete materials [29].

Furthermore, the FBM beam showed an increase in deflections of 29.63% at ultimate load levels compared to the FBC beam. The FBM beam's substantial deflections at maximum load show high ductile behavior, which may provide enough warning before the complete

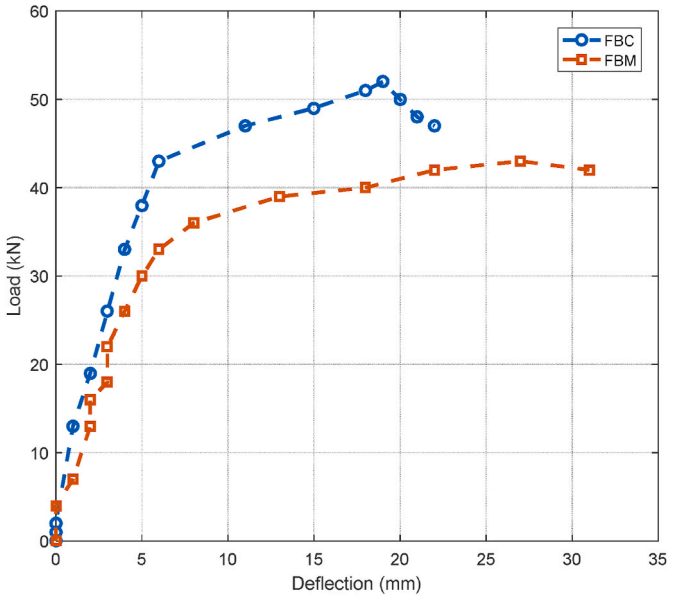

Fig. 10. Load-deflection curve.

collapse. This rise in deflection of FBM beam can be attributed to the inclusion of 5% of coconut shell particles which indicates that coconut shell particles have a high strain capacity [1]. The greater deflection is most likely owing to the CSP's low elastic modulus, which allows for improved energy absorption [38]. It can also be shown that the FBC beam behaves linearly at low loads, whereas the FBM beam differs little. This implies that the FBM beam began cracking earlier than the control. The FBC and FBM beams had a maximum of 19 mm and 27 mm deflections at ultimate loads. The finding of this study is in line with previous research [29–31].

Moreover, the ductility values of the FBC and FBM beams are also shown in Table 4. The displacement ductility ratio is calculated as ($\Delta u/\Delta y$), where Δu is the ultimate moment deflection, and Δy is the yields deflection. In general, a structural member with a high ductility ratio may withstand substantial deflections before failing. The ductility ratio for all beams was greater than 3, indicating relatively excellent ductility [32]. The ductility ratio of FBM was likewise found to be 8.8% greater than that of the control beam. As indicated by the ACV and AIV value tests (Section 2.1.1), as well as the presence of fiber on the CSP's outer surface, which may have contributed to the material's good ductility. According to the literature, structural members with displacement ductility in the range of 3–5 have appropriate ductility and can be employed for structural members subjected to substantial displacements, such as abrupt earthquake stresses [33]. Hence, incorporating the small amount of CSP (5% CSP) with a maximum aggregate size of 20 mm increased the ductility performance of FBM compared to control. The results of this research are consistent with those of Gunasekaran et al. [1] but differ with the introduction of CSA and the amount of CSP particle size grading.

3.3.2. Crack pattern, details, and mode of failure

After a thorough visual inspection, Fig. 11 displays the tested beams' crack pattern and failure mechanisms. The cracks were generally localized to the mid-section of the beams. Table 5 also provides load at first crack, ultimate crack, and failure mode.

The crack development was enhanced in the FBM beams compared to the FBC beams. It was observed that the first crack load for the FBM beam was lower than the control beam, which entails that FBM started cracking at lower loads (Table 5). More so, the presence of CSP caused an increase in mid-span deflection (Fig. 11 b), which is thought to be the cause of such behavior. Given the loading point location, flexure failure was the form of failure for both beams. There were more cracks with branches in FBM beams (Fig. 11 b), whereas control (FBC) beams had vertical cracks that were wide with no branching.

When the microcracks preceding the crack tip are halted, greater energy is required to propagate the crack [34]. Branching of fractures and redistribution of stresses, accompanied by a failure phase, are observed to result in concrete's ductile performance [35]. The addition of coconut shell particles seems to limit the development of wide cracks opening (Fig. 11 b). This is in line with the findings of Ismail and Hassan [36], who discovered that conventional concrete exhibits wider cracks than tire rubber as a lightweight aggregate in concrete.

At ultimate load levels, Table 6 displays the crack specifics, which include the overall number of cracks, crack growth, and crack spacing. The total number of cracks in the FBM beam rose when the load was increased. The same correlation was observed with the FBC beam. The FBC and FBM beams had a total of four (4) and eight (8) cracks, respectively. At maximal load levels, the total number of cracks in the FBM beam was twice that of the control (FBC) beam. The addition of 10% CSA in the FBM beam was anticipated to be sufficient to boost strength (as shown in Fig. 9) and reduce the frequency of cracks, but it had no positive effect due to the pozzolan in the ash not being activated at 28 days of curing. CSP concrete with 10% CSA has a considerable number of clustered cracks, as evidenced by the low load deflection graph (Fig. 10). According to this theory, the large strain rate difference between coconut shell particles and concrete is caused by coconut shells' high Poisson ratio and low modulus [1].

An increase in the rate of crack growth was seen as both beams were loaded up to failure. The crack propagation in both beams differs with the same loading position. Compared to the FBC beam, the FBM beam had a higher rate of crack formation. This is because the FBM beam reduced modulus of elasticity compared to control. Additionally, the presence of fibers on one side of the CSP could have aided in the propagation of cracks in the FBM beam. At the maximum load level, the FBM and FBC beams showed crack propagation of 183 mm and 165 mm, respectively. The crack spacing reduces as the number of cracks and loads are increased. The crack spacing in control (FBC) beam was greater than that of the FBM beam. FBC and FBM beams had a typical crack spacing of 85 and 66 mm. The smaller crack spacing in the FBM is owing to the fact that the FBM has more cracks than the FBC beam.

3.3.3. Concrete and steel strain

Concrete and steel strains were measured for FBC and FBM beams. Compressive and tensile strains are represented by the negative and positive concrete strains in Fig. 12. The maximum compressive strains for FBC and FBM were −0.0025 and −0.0029, respectively. The greatest strains in the tensile zone were 0.00042 for FBC and 0.0024 for FBM, respectively. Strain gauges were installed on the top and bottom middle surfaces of the beams for recording strain. The findings show that the strains increased as well when the stress was increased. Strain gauges placed on the upper surface of both beams' middle section revealed the highest strain.

In Fig. 12, the compression and tensile zones of the FBM beam had the maximum negative and positive load-strain slopes compared to the FBC beam. The fact that CSP has a low modulus of elasticity and a weak particle bond at the inner surface explains this phenomenon. Unfortunately, due to the limited curing period, 10% of CSA could not contribute to the strain capacity of the FBM beam since pozzolan content in the ash was not activated. The FBM beam had more strain than the FBC in tension steel, as seen in Fig. 13. FBM beam tension-steel exhibits

Table 4
Ductility ratio.

SI No	Specimen ID	Deflection at yield (mm)	Deflection at failure (mm)	Ductility ratio ($\Delta u/\Delta y$)
1	FBC	6	19	3.1
2	FBM	8	27	3.4

(a) FBC (Control)

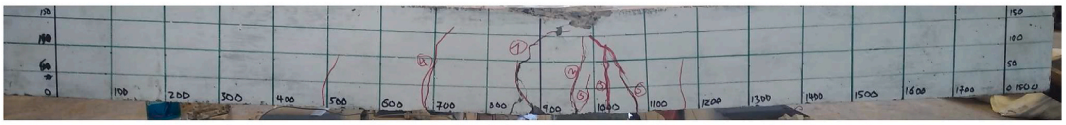

(b) FBM (10% CSA and 5% CSP5-20)

Fig. 11. Crack pattern and failure mode for control and modified concrete beams.

Table 5
Crack loads and failure mode.

SI No	Specimen ID	First Crack Load (KN)	First Crack Deflection (mm)	Ultimate Load (KN)	Ultimate Load Deflection (mm)	Failure mode
1	FBC	26	3	52	19	Flexure
2	FBM	18	2	43	27	Flexure

Table 6
Crack details.

SI No	Specimen ID	Number of cracks (Ultimate)	Crack Propagation (Ultimate)	Crack Spacing (Ultimate)
		NO	mm	mm
1	FBC	4	165	85
2	FBM	8	183	66

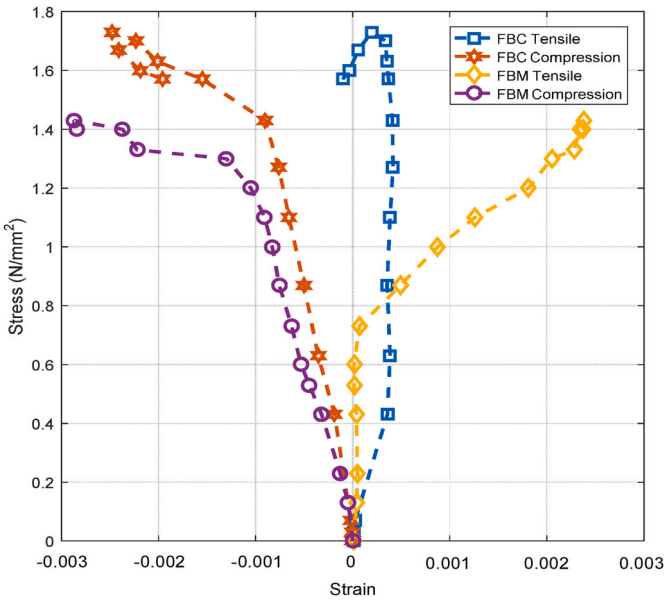

Fig. 12. Concrete strain (tension and compression).

significant strain due to the limited curing period of CSA, smooth surface of the inner part, and low modulus of elasticity of CSP. The strain in concrete and steel results for FBM are compatible with previous studies' findings [28,37].

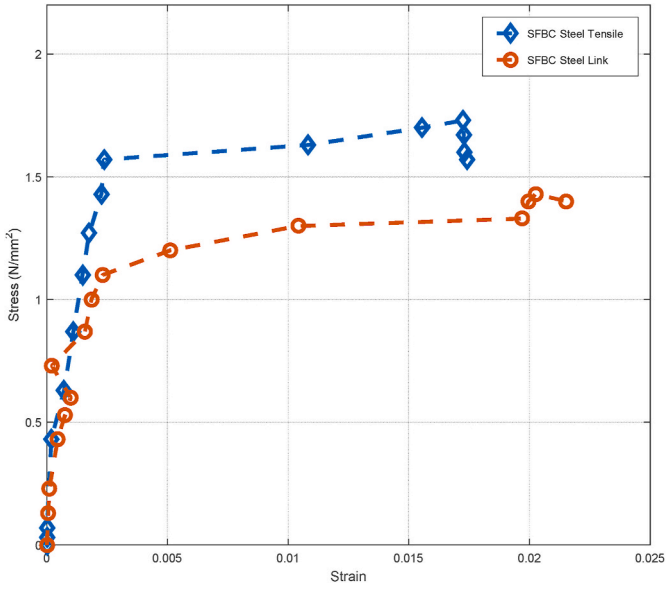

Fig. 13. Steel strain (main reinforcement).

3.4. Flexural, shear, and deformation

3.4.1. Load-deflection and ductility behavior

Fig. 14 illustrates the load-central deflection behavior of the control beam (SFBC) and modified beam (SFBM) tested for flexural, shear, and deformation. The loading point was repositioned to a distance of 200 mm from the support with a shear span to an effective depth ratio of 1.24 in order for the beams to fail in bending and shear. There were three portions captured in Fig. 14 curves, with the first occurring until cracking, the second until yielding, and finally until failure. As the load reduced, all tested beams exhibited continuous deflection. A 7.4% reduction in ultimate failure loads was found in the SFBM beam with 5% CSP and 10% CSA combined when compared to the SFBC beam. The ultimate deflection points for the SFBM beam appear to be higher than those for the FBC beam.

Fig. 14 shows that SFBM with CSA sustained a lower load than SFBC. This phenomenon appears to be caused by the smoothness of the inner portion of CSP, which causes sliding in concrete and hence a lower modulus of elasticity. Coconut shell particles as aggregates decrease aggregate interlock even further, contributing 35–50% of the beam shear capacity. More specifically, the addition of 10% CSA resulted in a reduction in beam stiffness, as evidenced by the reduced load-deflection slope in Fig. 16. This could be explained by a decrease in beam bonding caused by adhesion loss at the steel-concrete interface [38]. Longer

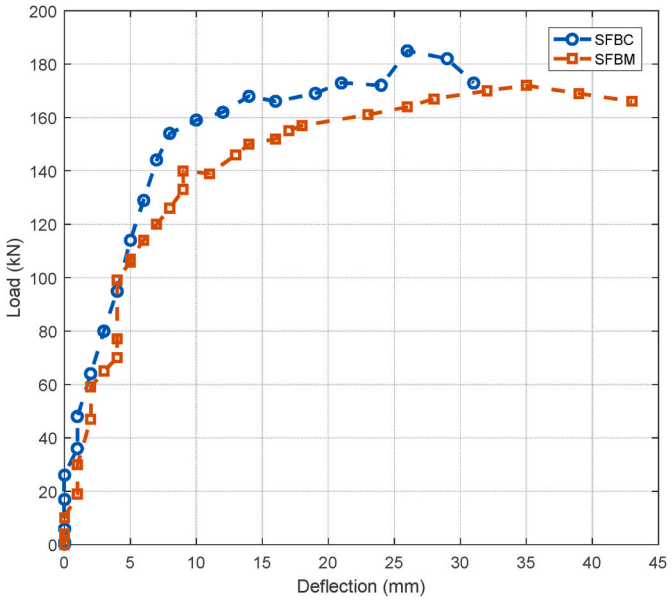

Fig. 14. Load-deflection curve.

concrete curing times can result in a reasonable increase in adhesion in concrete containing CSA, as illustrated in Fig. 9.

Table 7 shows the improvement in ductility ratio for SFBM beam with 10% CSA versus SFBC beam. The ductility ratio of the SFBM beam increased by 9.5% as compared to the SFBC beam. The reduced load yielding failure was attributable to the SFBM beam's lower section stiffness than the SFBC beam. Such a phenomenon was discussed in the previous section on beams subjected to flexural and ductility. It is clear that when loads are placed close to the supports, the ultimate load of the beams improves, and the ductility ratio decreases under the same reinforcement settings as the prior beams evaluated for flexural and ductility.

3.4.2. *Crack pattern, details, and mode of failure*

Fig. 15 demonstrates the flexural and shear failure modes of SFBC and SFBM concrete beams. The loading point was repositioned 200 mm closer to the support, with the same reinforcement design and arrangement for beams that tested for flexural and deformation. Steel yielded, which was followed by vertical and diagonal cracks, as well as concrete crushing, as seen in Fig. 15.

The fact that the SFBC beam had fewer cracks than the SFBM beam suggested that the SFBM beam had better strain distribution. This behavior was also seen in beams that were tested for flexural and deformation described earlier. It was suggested that increasing the rigidity of the control beam might lessen the number of cracks. However, both had more cracks than beams that failed in flexure. According to this observation, placing the load 200 mm from the supports affected the number of cracks.

The addition of CSP permitted the SFBM beam to experience considerable deflections and a more quantity of cracks before final failure. The inclusion of CSP reduces the modulus of elasticity, explaining this behavior [9]. This type of behavior is desired because it reduces seismic damage by providing enough warning to building occupants during earthquakes [39]. Table 8 also shows the first crack load, first crack deflection, ultimate loads, ultimate deflection, and failure mode.

Table 7
Ductility ratio.

SI No	Specimen ID	Deflection at yield (mm)	Deflection at failure (mm)	Ductility ratio ($\Delta u/\Delta y$)
1	SFBC	14	26	1.9
2	SFBM	17	35	2.1

Following the failure of the beams, the overall number of cracks in the SFBC beam was twelve (12), while the maximum count of cracks in the SFBM beam was fifteen (15), as seen in Table 9. At maximum load levels, the overall number of cracks in the SFBM beam was three (3) cracks higher than in the SFBC beam. When the loading point was shifted 200 mm closer to the support, the number of total cracks in both beams was also higher than in the beams tested for flexural performance. This is due to the loading point close to the beam's edge, which increases load capacity.

During loading, crack propagation was monitored from the bottom to the top of both beams and was measured after the beams had totally failed. As the load increased, crack propagation increased in all beams. The crack propagation was greater in the SFBM beam than in the control beam under the same shear span to effective depth ratio. The crack propagation lengths in SFBC and SFBM beams were 153 and 178 mm, respectively.

The combined inclusion of 5% CSP and 10% CSA in the SFBM beam reduced the maximum crack spacing by 13.5% compared to the SFBC. One explanation for this behavior could be an enhancement in strain distribution in SFBM, which increases the number of cracks. Other researchers [9,40] found that maximum crack spacing was reduced palm kernel concrete and fly ash concrete with coconut shell coarse aggregate compared to control concrete.

Furthermore, because of the low elastic modulus of the CSP, the addition of CSP in SFBM beams has been shown to reduce crack spacing [41]. Beam ductility is connected with a rise in the number of cracks, a decrease in crack spacing, and a decrease in crack width [10].

3.4.3. *Strain in tension steel, links, and concrete*

Figs. 16 and 17 demonstrate the fluctuation of strains in concrete (tension strain, compression strain, and shear strain) and steel reinforcements (tension steel and shear links) for SFBC and SFBM beams. The tensile strain, compressive strain, and strain along the line of shear of the beams with and without the combination of CSA and CSP show the linearity from the start of the experiment until the formation of cracks, beam failure, and sliding of the strain gauges in the concrete (Fig. 16). As the stress was increased, the concrete strain for the SFBC and SFBM beam soared. Fig. 17 shows a disparity in the slopes of SFBC and SFBM concrete strain in compression, shear, and tension, which could be caused by strain gauge sliding during loading. Another probable cause could be concrete straining due to persistent load application. It was observed that SFBM beam concrete strain (compression and tensile) yielded a larger strain than the SFBC beam. The low modulus of elasticity of SFBM is responsible for its high concrete strain in compression and tension. Fig. 16 also shows that the strain occurring perpendicular to the shear line was larger for the SFBC beam than the SFBM beam. The smoothness of the interior portion of the CSP affects the interlocking of the aggregates, reducing the shear resistance. Furthermore, because the pozzolan content of the CSA in the SFBM beam was not activated during the 28-day curing period, it is possible that it did not play a substantial role in improving the bond between the aggregates and the cement matrix.

Fig. 17 shows that the SFBM with 10% CSA and 5% CSP tension reinforcement and shear link displayed higher strains and yielded before the SFBC beam shear link strain. The shear link strain graph of the SFBM beam did not display a linear behavior but rather zigzagged, as shown in Fig. 17. This behavior could also result from a weak bond between CSP inner section and the cement matrix, allowing the links to carry most of the shear loads. The main reinforcement of the SFBM beam revealed higher concrete strains before failure than the control beam (SFBC). The higher concrete stresses in the SFBM beam indicate a stronger bond between the longitudinal reinforcement and the CSP. The high strain capacity is comparable to the ductility properties of CSP in SFBM beam.

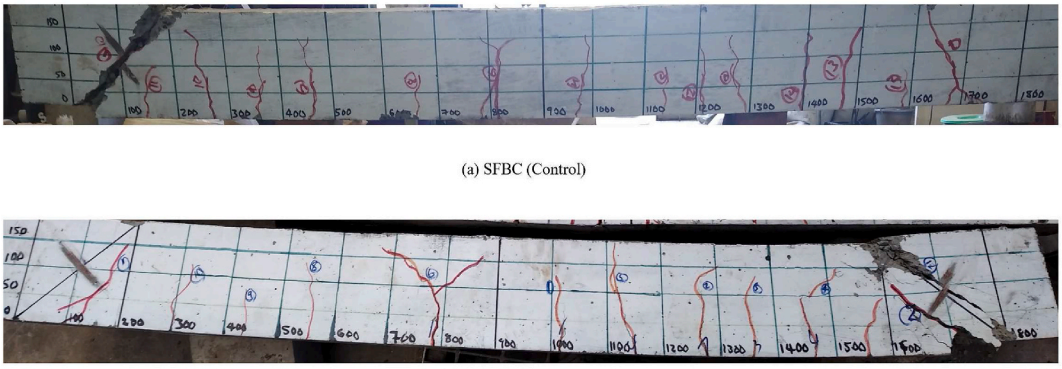

(a) SFBC (Control)

(b) SFBM (10% CSA and 5% CSP5-20)

Fig. 15. Crack pattern and failure mode for control and modified concrete beams.

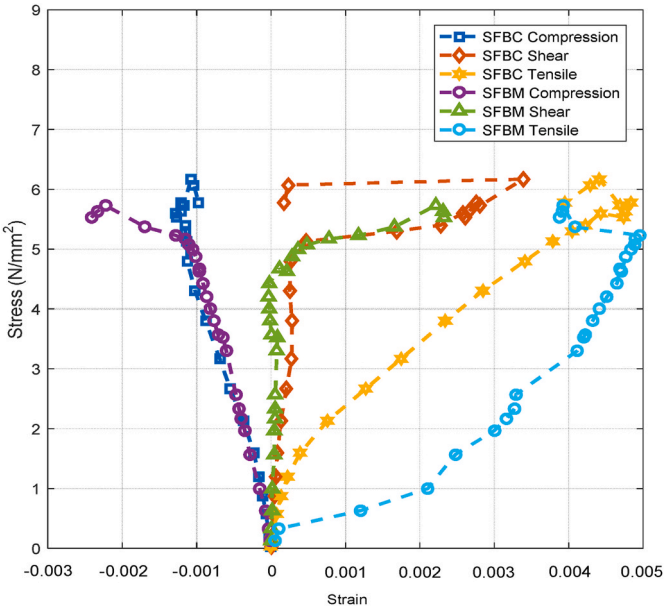

Fig. 16. Concrete strain (tension, compression and shear).

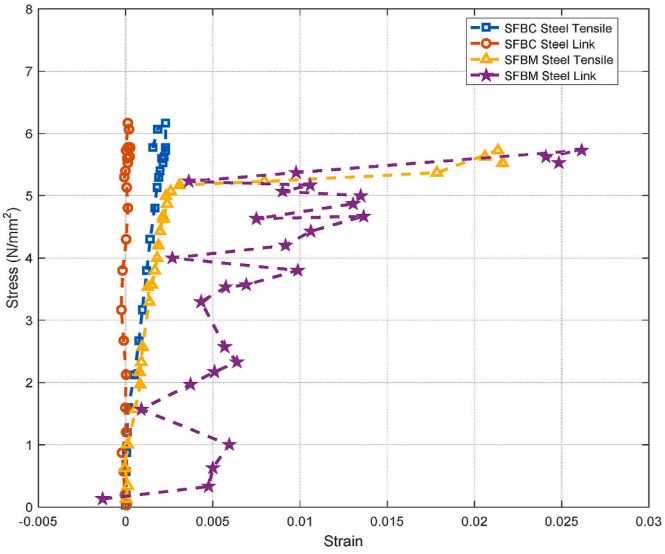

Fig. 17. Steel Strain (main reinforcement and links).

Table 8
Crack loads and failure mode.

SI No	Specimen ID	First Crack Load (KN)	First Crack Deflection (mm)	Ultimate Load (KN)	Ultimate Load Deflection (mm)	Failure mode
1	SFBC	95	3	185	26	Shear – flexure
2	SFBM	70	4	172	35	Shear – flexure

Table 9
Crack details.

SI No	Specimen ID	Number of cracks (Ultimate)	Crack Propagation (Ultimate)	Crack Spacing (Ultimate)
		NO	mm	mm
1	SFBC	12	153	126
2	SFBM	15	178	109

3.4.4. *Validation of shear capacity experimented*

Reinforced concrete members' shear behavior is more complex than its flexural behavior. Many factors influence shear capacity, including non-linearity, non-homogeneity, reinforcement, and so on [42]. The ultimate shear capacity of SFBC and SFBM in this research was achieved by converting the ultimate load to shear force. With the aid of Eq. (1), the experimental shear capacity of the beams tested for flexural and shear performance is shown. Where P denotes the ultimate load, and V represents the shear force.

$$V = \frac{P}{2} \tag{1}$$

Beam shear capacity is also referred to as its shear force. The experimental shear strength of the beams examined is compared to the shear capacity reported in the literature captured in Fig. 18. As illustrated in Fig. 18, the shear capacities of SFBC and SFBM are larger than those reported [41,43,44]. The rationale for the high shear capacity is that the shear span to effective depth ratio was chosen to be 1.24 due to the fact that the loading point was relocated 200 mm from the support. With a low shear span to effective depth ratio, high shear strength is possible. Additionally, when compared to the shear strength result obtained by Sinkhonde et al. [43] under a similar loading position, SFBM with 10% CSA demonstrated a greater shear strength. The increased shear strength is due to the inclusion of the particle size and quantity of CSP in the SFBM beam, thus occupying less surface area. As illustrated in

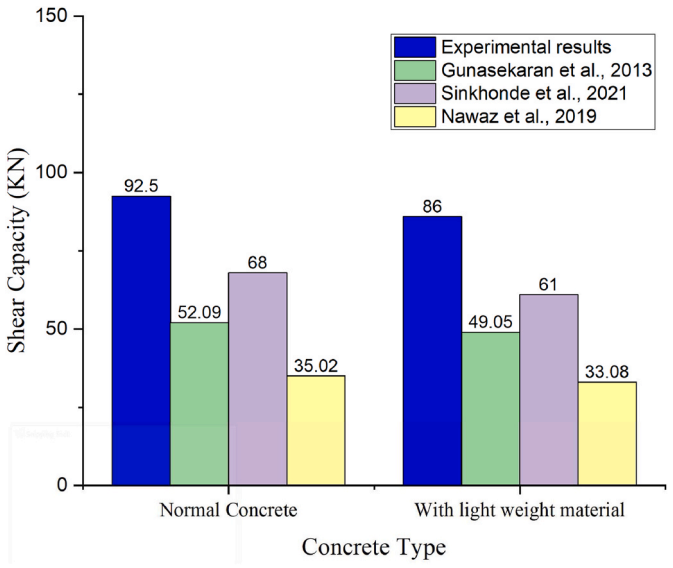

Fig. 18. Control and Modified concrete beams shear capacity vs. shear capacity from Literature.

Fig. 18, increasing the amount of lightweight material reduces the shear capacity of a beam.

4. Conclusions

The findings given in this research led to the following conclusions.

1. When flexural tests were performed on FBM beams containing 10% CSA and 5% CSP, the ductility ratio improved by 8.8% when compared to FBC concrete beam. Only a 17.3% drop in flexural load was required to demonstrate this gain in ductility.
2. Compared to the SFBC concrete beam, the SFBM beam containing 10% CSA and 5% CSP tested for flexure, ductility, and shear showed a lower ductility value than beams tested for only flexural and ductility. Placing the loading point close to support can decrease ductility performance and thus increase the shear load. Both concrete investigated had higher experimental shear capacities than the reference literature.
3. Incorporating 10% CSA and 5% CSP in reinforced concrete beams makes it feasible to produce increased ductility without considerably reducing the ultimate failure load, which has been highlighted as a promising option for seismic applications.
4. When flexural and deformation tests were performed on FBM containing 10% CSA, branching cracks predominated over straight cracks when compared to FBC.
5. Strain behavior of FBM and SFBM concrete beams containing 10% CSA and 5% CSP tested for flexure, ductility, shear, and cracking behavior exhibit larger strain than control beams (FBC and SFBC).
6. The findings from the research shows that a reinforced coconut shell concrete beam with the limited pozzolanic reaction of CSA can still perform structurally when subjected to apply loads.

Credit author statement

Trokon Cooper Herring: Conceptualization, Methodology, Validation, Formal analysis, Investigation, Resources, Writing – original draft, Visualization.: Timothy Nyomboi: Conceptualization, Methodology, Investigation, Resources, Data curation, Writing – review & editing, Supervision.: Joseph N. Thuo: Conceptualization, Methodology, Investigation, Resources, Writing – review & editing, Supervision.

Declaration of competing interest

The authors declare that they have no known competing financial interests or personal relationships that could have appeared to influence the work reported in this paper.

Acknowledgements

Sincere appreciation to Pan African University for funding the research. The authors would also like to thank the Jomo Kenyatta University of Agriculture and Technology for providing laboratory equipment and technical assistance during this research.

References

[1] K. Gunasekaran, R. Annadurai, P.S. Kumar, Study on reinforced lightweight coconut shell concrete beam behavior under flexure, Mater. Des. 46 (Apr. 2013) 157–167, https://doi.org/10.1016/j.matdes.2012.09.044.
[2] M.Z. Jumaat, U.J. Alengaram, H. Mahmud, Shear strength of oil palm shell foamed concrete beams, Mater. Des. 30 (6) (2009) 2227–2236.
[3] K. Wang, in: Proceedings of the International Workshop on Sustainable Development and Concrete Technology, Center for Transportation Research and Education Iowa State University, Beijing, China, 2004. May 20-21, 2004.
[4] H. Weigler, S. Karl, Structural lightweight aggregate concrete with reduced density—lightweight aggregate foamed concrete, Int. J. Cem. Compos. Lightweight Concr. 2 (2) (1980) 101–104.
[5] K. Gunasekaran, P.S. Kumar, Lightweight concrete using coconut shell as aggregate, in: Proceedings of the ICACC-2008. International Conference on Advances in Concrete and Construction, Hyderabad, India, 2008, pp. 7–9.
[6] L. Thangasamy, G. Kandasamy, Behavior of steel–coconut shell concrete–steel composite beam without and with shear studs under flexural load, Materials 13 (11) (May 2020), https://doi.org/10.3390/ma13112444.
[7] L. Thangasamy, G. Kandasamy, Behavior of steel–coconut shell concrete–steel composite beam without and with shear studs under flexural load, Materials 13 (11) (May 2020), https://doi.org/10.3390/ma13112444.
[8] K. Gunasekaran, R. Annadurai, P.S. Kumar, Long term study on compressive and bond strength of coconut shell aggregate concrete, Construct. Build. Mater. 28 (1) (Mar. 2012), https://doi.org/10.1016/j.conbuildmat.2011.08.072.
[9] R. Prakash, R. Thenmozhi, S.N. Raman, Mechanical characterisation and flexural performance of eco-friendly concrete produced with fly ash as cement replacement and coconut shell coarse aggregate, Int. J. Environ. Sustain Dev. 18 (2) (2019) 131–148.
[10] U.J. Alengaram, M.Z. Jumaat, H. Mahmud, Ductility behaviour of reinforced palm kernel shell concrete beams, Eur. J. Sci. Res. 23 (3) (2008) 406–420.
[11] M.K. Ismail, A.A.A. Hassan, Ductility and cracking behavior of reinforced self-consolidating rubberized concrete beams, J. Mater. Civ. Eng. 29 (1) (2017), 04016174.
[12] D. Sinkhonde, A. Rimbarngaye, B. Kone, T.C. Herring, Representativity of morphological measurements and 2-d shape descriptors on mineral admixtures, Results Eng. 13 (Mar. 2022) 100368, https://doi.org/10.1016/j.rineng.2022.100368.
[13] N. Bheel, S. Sohu, A.A. Jhatial, N.A. Memon, A. Kumar, Combined effect of coconut shell and sugarcane bagasse ashes on the workability, mechanical properties and embodied carbon of concrete, Environ. Sci. Pollut. Control Ser. (Aug. 2021), https://doi.org/10.1007/s11356-021-16034-3.
[14] A.J. Adeala, J.O. Olaoye, A.A. Adeniji, Potential of coconut shell ash as partial replacement of ordinary Portland cement in concrete production, Int. J. Eng. Sci. Invent. 9 (1) (2020) 47–53.
[15] N. Bheel, S.K. Mahro, A. Adesina, Influence of coconut shell ash on workability, mechanical properties, and embodied carbon of concrete, Environ. Sci. Pollut. Control Ser. 28 (5) (Feb. 2021), https://doi.org/10.1007/s11356-020-10882-1.
[16] S. Popovics, Concrete Materials Properties, Specifications and Testing, second ed., Noyes Publications, New Jersey, USA, 1992.
[17] British Standard Institution, "BS EN 1097 (2013)- Test for Mechanical and Physical Properties of Aggrgeates, BSI Standards Limited, 2013.
[18] BS 882, SPECIFICATION FOR AGGREGATES FROM NATURAL SOURCES FOR CONCRETE, British Standards Institution, London, 1992.
[19] BS 1881-103, Testing Concrete. Method for Determination of Compacting Factor, BSI, Lond, UK, 1993.
[20] BS 1881-102, Testing Concrete. Method for Determination of Slump, BSI, London, UK, 1983.
[21] BS EN ISO 6892-1, Metallic Materials. Tensile Testing. Method of Test at Room Temperature, BSI, UK, London, 2019.
[22] BS EN 10080, Steel for the Reinforcement of Concrete. Weldable Reinforcing Steel, BSI, London, 2005. *General*. UK.
[23] J.N. Mwero, S.O. Abuodha, Residual strength of reworked steel reinforcement bars, Int. J. Sci. Res. Publ. (IJSRP) 8 (6) (Jun. 2018), https://doi.org/10.29322/IJSRP.8.6.2018.p7811.
[24] BS EN 12390-5, Testing Hardened Concrete. Flexural Strength of Test Specimens, BSI, London UK, 2009.

[25] K. Gunasekaran, R. Annadurai, P.S. Kumar, Long term study on compressive and bond strength of coconut shell aggregate concrete, Construct. Build. Mater. 28 (1) (Mar. 2012), https://doi.org/10.1016/j.conbuildmat.2011.08.072.
[26] Z. Bayasi, P. Soroushian, Optimum use of pozzolanic materials in steel fiber reinforced concrete, Transport. Res. Rec. (1990) 25–30.
[27] R. Tomar, K. Kishore, H. Singh Parihar, N. Gupta, A comprehensive study of waste coconut shell aggregate as raw material in concrete, Mater. Today Proc. 44 (2021) 437–443, https://doi.org/10.1016/j.matpr.2020.09.754.
[28] K. Gunasekaran, R. Annadurai, P.S. Kumar, Study on reinforced lightweight coconut shell concrete beam behavior under flexure, Mater. Des. 46 (Apr) (2013), https://doi.org/10.1016/j.matdes.2012.09.044.
[29] S. Haruna, M. Lakshmipathy, Ductility behaviour of bamboo reinforced coconut shell concrete beams, Int. J. Sci. Eng. Res. 3 (5) (2014) 1–7.
[30] U.J. Alengaram, M.Z. Jumaat, H. Mahmud, Ductility behaviour of reinforced palm kernel shell concrete beams, Eur. J. Sci. Res. 23 (3) (2008) 406–420.
[31] D.C.L. Teo, M.A. Mannan, J. v Kurian, Flexural behaviour of reinforced lightweight concrete beams made with oil palm shell (OPS), J. Adv. Concr. Technol. 4 (3) (2006) 459–468.
[32] D.C.L. Teo, M.A. Mannan, J. v Kurian, Flexural behaviour of reinforced lightweight concrete beams made with oil palm shell (OPS), J. Adv. Concr. Technol. 4 (3) (2006) 459–468.
[33] S.A. Ashour, Effect of compressive strength and tensile reinforcement ratio on flexural behavior of high-strength concrete beams, Eng. Struct. 22 (5) (2000) 413–423.
[34] T.M. Fayyad, J.M. Lees, Experimental investigation of crack propagation and crack branching in lightly reinforced concrete beams using digital image correlation, Eng. Fract. Mech. 182 (Sep. 2017) 487–505, https://doi.org/10.1016/j.engfracmech.2017.04.051.
[35] I. Vegt, V.K. Breugel, J. Weerheijm, Failure mechanisms of concrete under impact loading," *Fracture Mechanics of Concrete and Concrete Structures*, FraMCoS-6 1 (2007) 579–587.
[36] M.K. Ismail, A.A.A. Hassan, Shear behaviour of large-scale rubberized concrete beams reinforced with steel fibres, Construct. Build. Mater. 140 (Jun. 2017) 43–57, https://doi.org/10.1016/j.conbuildmat.2017.02.109.
[37] M.A. Rashid, M.A. Mansur, Reinforced high-strength concrete beams in flexure, ACI Struct. J. 102 (3) (2005) 462.
[38] M.I. Mousa, Flexural behaviour and ductility of high strength concrete (HSC) beams with tension lap splice, Alex. Eng. J. 54 (3) (Sep. 2015) 551–563, https://doi.org/10.1016/j.aej.2015.03.032.
[39] A.K.H. Kwan, J.C.M. Ho, Ductility design of high-strength concrete beams and columns, Adv. Struct. Eng. 13 (4) (2010) 651–664.
[40] U. Johnson Alengaram, M. Z. Jumaat, H. Mahmud, and M. M. Fayyadh, "Shear behaviour of reinforced palm kernel shell concrete beams," Construct. Build. Mater., vol. 25, no. 6, pp. 2918–2927, Jun. 2011, doi: 10.1016/j.conbuildmat.2010.12.032.
[41] K. Gunasekaran, R. Annadurai, P.S. Kumar, Study on reinforced lightweight coconut shell concrete beam behavior under shear, Mater. Des. 50 (Sep. 2013), https://doi.org/10.1016/j.matdes.2013.03.022.
[42] S. Nagajothi, S. Elavenil, Shear Prediction of geopolymer concrete beams using Basalt/Glass FRP bars, J. Adv. Concr. Technol. 19 (3) (2021) 216–225.
[43] D. Sinkhonde, R. O. Onchiri, W. O. Oyawa, and J. N. Mwero, "Ductility performance of reinforced rubberised concrete beams incorporating burnt clay powder," Heliyon, vol. 7, no. 11, p. e08310, Nov. 2021, doi: 10.1016/j.heliyon.2021.e08310.
[44] W. Nawaz, et al., Experimental study on the shear strength of reinforced concrete beams cast with Lava lightweight aggregates, Archiv. Civ. Mech. Eng. 19 (4) (Aug. 2019) 981–996, https://doi.org/10.1016/j.acme.2019.05.003.